The cell developmental atlas of human embryonic temporomandibular joint

Qianqi Zhu
Nantong University Affiliated Hospital: Affiliated Hospital of Nantong University
Miaoying Tan
Nantong University Affiliated Hospital: Affiliated Hospital of Nantong University
Chengniu Wang
Nantong University Medical School
Yufei Chen
Nantong University Medical School
Chenfei Wang
Nantong University Affiliated Hospital: Affiliated Hospital of Nantong University
Junqi Zhang
Nantong University Affiliated Hospital: Affiliated Hospital of Nantong University
Yijun Gu
Nantong University Affiliated Hospital: Affiliated Hospital of Nantong University
Yuqi Guo
Nantong University Affiliated Hospital: Affiliated Hospital of Nantong University
Jianpeng Han
Nantong University Affiliated Hospital: Affiliated Hospital of Nantong University
Lei Li
Nantong University Affiliated Hospital: Affiliated Hospital of Nantong University
Rongrong Jiang
Nantong University Affiliated Hospital: Affiliated Hospital of Nantong University
Xudong Fan
Nantong University Affiliated Hospital: Affiliated Hospital of Nantong University
Huimin Xie
Nantong University Affiliated Hospital: Affiliated Hospital of Nantong University
Liang Wang
Nantong University Affiliated Hospital: Affiliated Hospital of Nantong University
Zhifeng Gu
Nantong University Affiliated Hospital: Affiliated Hospital of Nantong University
Dong Liu
Nantong University
Jianwu Shi

Nantong University Medical School

Xingmei Feng (xingmeifeng@ntu.edu.cn)

Affiliated Hospital of Nantong University https://orcid.org/0000-0002-2063-5885

Research Article

Keywords: TMJ, Human embryonic cells, Cell transcriptomics, Gene expression

Posted Date: November 1st, 2022

DOI: https://doi.org/10.21203/rs.3.rs-2174997/v1

Abstract

Background: The temporomandibular joint (TMJ) is a complex joint consisting of the mandibular condyle, temporal articular surface, and articular disc. The functions of mastication, swallowing and articulation are accomplished by the movements of the TMJ. To date, the TMJ has been studied more extensively, but the study of the TMJ is limited by the type of TMJ cells, their differentiation, and their interrelationship during growth and development is unclear. The aim of this study is to establish a molecular cellular developmental atlas of the human TMJ by single-cell RNA sequencing, which will contribute to understanding and solving.

Results: We performed a comprehensive transcriptome analysis of TMJ tissue from 3- and 4-month-old human embryos using single-cell RNA sequencing. A total of 15,624 cells were captured and the gene expression profiles of 15 cell populations in human TMJ were determined, including 14 known cell types and a previously unknown cell type named "transition state cells (TSCs)". Immunofluorescence assays confirmed that TSCs are not the same cell cluster as mesenchymal stem cells (MSCs). Pseudotime trajectory and RNA velocity analysis showed that MSCs transformed into TSCs, and TSCs further differentiated into tenocytes, hypertrophic chondrocytes and osteoblasts. In addition, chondrocytes were detected only in 4-month-old human embryonic TMJ.

Conclusions: Our study provides an atlas of the earlier cellular development of human embryonic TMJ tissue, which will contribute to a deeper understanding of the pathophysiology of TMJ tissue during repair and ultimately help to solve clinical problems.

Introduction

During human embryonic development, abnormal chondrogenesis of TMJ condyle can lead to the malformation of the oral and maxillary system, abnormal respiratory and masticatory dysfunction[1,2]. The dysplasia of the embryonic TMJ could even lead to the occurrence of congenital TMJ diseases in human adults. The TMJ is a complex joint including mandibular condyle, temporal articular surface, articular disc, etc[1,3]. The functions of mastication, swallowing, and articulation are accomplished by TMJ movement[2,4].

The development of human embryonic TMJ can be divided into three periods. The first period is the blastematic stage, ranging from 7 to 8 weeks of gestation. The second period is the cavitation stage, which begins by 9 weeks and is completed by 11 weeks in a fetus. The last period is the maturation stage, which begins by 12 weeks and lasts until the completion of embryonic development[2,5]. So far, the majority of studies on the human embryonic TMJ are still limited to pathological and imaging levels. At present, there is no study on the cell types and differentiation relationship of human embryonic TMJ.

Many key genes and transcription factors were reported to participate in the differentiation of chondrocytes and osteoblasts. The common mesenchymal progenitors of chondrocytes and osteoblasts

can simultaneously express Sox9 and Runx2[6]. The cells' differentiation direction toward chondrocyte or osteoblast depends on the expression of Sox9 and Runx2[7]. Sox9 regulates the differentiation of chondrocytes[8]. Runx2 is expressed in hypertrophic chondrocytes and promotes the expression of Col10a1 and Mmp13[9]. Runx2 also promotes the differentiation of osteoblast by regulating the expression of Osx[10]. Osx transactivates Col1a1, which is essential for the differentiated osteoblasts. Therefore, Osx is essential for preosteoblast differentiation[10]. Moreover, many signaling pathways were reported to participate in the differentiation of bone cells. The Indian Hedgehog (IHH) signaling pathway can promote chondrocytic to hypertrophic terminal differentiation[11]. Conversely, the parathyroid hormone-related peptide (PTHrP) signaling pathway can prevent chondrocytes from premature differentiation[12]. Many other signaling pathways including PTN[13], BMP[14], FGF[15], CXCL[16], MSTN[17] and GH[18] were related to the differentiation of chondrocytes and osteoblasts in the previous studies. In short, exploring the key genes, transcription factors and signaling pathways are of great significance for understanding the development and differentiation of human embryonic TMJ cells.

In recent years, single-cell sequencing technologies have been used for investigating the cell types of tissue and the differentiation relationships among cell clusters. To investigate the cell types and differentiation relationship of human embryonic TMJ, we have accomplished the single-cell sequencing of 3 and 4-month-old human embryonic TMJ. To our knowledge, this is the first and earliest single-cell atlas of human embryonic TMJ. In this study, we described the cell types and differentiation relationship of human embryonic TMJ cells. This is of great significance for studying the function and differentiation relationship of cell clusters and the congenital TMJ diseases caused by the abnormal development of human embryonic TMJ.

Results

scRNA-Seq analysis of human embryonic TMJ cell types

In order to construct the cell development atlas of human embryonic TMJ, we have isolated the TMJ tissues during two early development phases: 7,052 cells from the 3-month-old TMJ and 9,572 cells from the 4-month-old TMJ. Following cell quality control (Fig. S1a), a total of 15,624 cells were clustered into 15 cell populations. We have annotated these 15 cell clusters, including satellite cells, MSCs, TSCs, tenocytes, myoblasts, endothelial cells, hypertrophic chondrocytes, erythrocytes, proliferating cells, leukocytes, pericytes, chondrocytes, schwann cells, osteoblasts and osteoclasts (Fig. 1a). Unexpectedly, we did not find a chondrocytes cluster in the 3-month-old TMJ. However, an obvious chondrocytes cluster appeared in the 4-month-old TMJ (Fig. 1b and 1c). The marker genes used for the annotation were shown (Fig. S1b). As a marker gene of chondrocytes cluster, the expression of THBS1 was illustrated (Fig. 1d). Immunofluorescence staining showed that THBS1 was expressed in the 4-month-old TMJ. THBS1 was not detected in the 3-month-old TMJ (Fig. S2a, 2b and Fig. 1e). The top 5 DEGs were illustrated in each cluster (Fig. S1c). GO analysis of each cluster was also shown (Fig. S1d).

Subpopulation analysis of TSCs

In this study, we identified a specific cell cluster of TSCs. Subpopulation analysis showed that TSCs was consisted of 5 subpopulations (Fig. 2a). The proportions of subpopulations were osteoblasts (67.9%), preosteoblasts (19.0%), hypertrophic chondrocytes (7.1%), chondrocytes (3.0%) and mesenchymal stem cells (2.9%), respectively (Fig. 2b). Five subpopulations were annotated on the reported cell markers (Fig. S1e). As marker genes, the expression of CAPN6 in MSCs and PTN in TSCs was illustrated, respectively (Fig. 2c and 2d). Immunofluorescence staining showed that CAPN6 and PTN were not colocalizated and expressed in the different cells of 3 and 4-month-old TMJ (Fig. S2c, 2d and Fig. 2e). These results showed that MSCs and TSCs existed in 3 and 4-month-old TMJ. These results also further confirmed that MSCs and TSCs were different cell types in human embryonic TMJ (Fig. S2c, 2d and Fig. 2e).

Monocle3 and RNA velocity analysis of cell differentiation relationships

To clarify the differentiation relationship among TMJ cells, the 15 TMJ cell clusters were calculated and divided into eight differentiation trajectories based on Monocle3 analysis. A clear differentiation pathway could be found among MSCs, TSCs, tenocytes, hypertrophic chondrocytes and osteoblasts (Fig. S3a). We further focused on the differentiation relationship among these five cell clusters. It is reasonable for assigning the MSCs cluster as the root in the pseudotime trajectory path. The differentiation relationships among these five cell clusters were determined. MSCs positioned as an origin and differentiated into TSCs. TSCs could further differentiate into tenocytes, hypertrophic chondrocytes and osteoblasts, respectively (Fig. 3a). The pseudotime analysis of 3 and 4-month-old TMJ cells were also shown (Fig. S3c). In addition, we used RNA velocity analysis to observe the extent and direction of MSCs, TSCs, tenocytes, hypertrophic chondrocytes and osteoblasts. The direction of arrows showed that MSCs and TSCs had a high degree of heterogeneity and were regarded as starting points to each direction of differentiation. Tenocytes, hypertrophic chondrocytes and osteoblasts have the uniform direction of arrows, suggesting that these three clusters have a stable state and seemed to be differentiated from TSCs (Fig. 3b). The RNA velocity analysis of the 15 TMJ cell clusters and the five cell clusters of the 3 and 4-month-old TMJ was also shown (Fig. S3b and 3d), and these results were consistent with monocle3 analysis. The expression of key genes which were related to the differentiation of chondrocytes and osteoblast were illustrated. These genes included RUNX2, SOX9, MMP13, SOST, VEGFA, COL10A1, MAF, CCDC80, and SYNE2 (Fig. 3c). Finally, we performed gene set enrichment analysis (GSEA) among MSCs, TSCs, tenocytes, hypertrophic chondrocytes and osteoblasts. GSEA analysis showed that the data set of WP_OSTEOBLAST_DIFFERENTIATION was highly enrichment between MSCs and TSCs. GOBP_BONE_DEVELOPMENT and GOBP_OSSIFICATION were highly enrichment between TSCs and osteoblasts. These results further demonstrated that MSCs can differentiate into TSCs, and TSCs have the potential ability to differentiate into osteoblasts (Fig. 3d).

CellChat analysis of signaling pathways in cell clusters differentiation

To analyze cell-cell interactions and underlying signaling pathways, we screened the known cell-cell communications using CellChat. Complex cell-cell interaction networks were found among the 15 cell clusters (Fig. 4a and Fig. S4a). Notably, CellChat-inferred FGF signaling pathway was highly enriched among MSCs, TSCs, tenocytes, hypertrophic chondrocytes and osteoblasts (Fig. 4b and Fig. S4b). We further determined FGF7-FGFR1 was the primary contributor to FGF signaling pathway (Fig. 4c). We further investigated the expression of the molecules involved in FGF7-FGFR1 and found that FGFR1 was mainly expressed in TSCs, tenocytes, hypertrophic chondrocytes and osteoblasts (Fig. S4c). Therefore, FGF7-FGFR1 is the major signaling pathway that mediates the cell-cell communications among MSCs, TSCs, tenocytes, hypertrophic chondrocytes and osteoblasts (Fig. 4d and Fig. S4d). Moreover, we also demonstrated the other key signaling pathways with the function of “identify Communication Patterns” in CellChat. During the outgoing communication patterns of secreting cells, TSCs, hypertrophic chondrocytes and osteoblasts were in Pattern 1. Pattern 1 contained the signaling pathways of PTN, THBS, ANGPTL, FGF, TENASCIN, CHAD, CADM, CDH, BSP, BMP, HSPG, OSM, ncWNT, RANKL, ACTIVIN, SEMA4, IL16, and DMP1. Meanwhile, the incoming communication patterns of target cells demonstrated that TSCs, hypertrophic chondrocytes and osteoblasts were in Pattern 1 and were regulated by FGF, EPHA, MIF, BMP, GRN, CXCL, MSTN, ADGRE5, RANKL, ACTIVIN, SEMA4, CNTN, PROS, SEMA6 and GH (Fig. 4e and Fig. S4e).

Transcription factors analysis in cells cluster differentiation

The binary regulon activity matrix was charted in Fig. 5a, SP9, SHOX2, TBX18, PLAGL1, PAX9 and SRY were turned on in MSCs. TCF7, DLX6, BCL11A, PRRX2 and MSX1 were turned on in TSCs. MKX, ETV4, DLX1, ALX4 and USF1 were turned on in tenocytes. FOXA2, TRPS1, SOX6, SIX3 and FOXA3 were turned on in hypertrophic chondrocytes. ZBTB7C, DLX3, IRX5 and TBX2 were turned on in osteoblasts. Strikingly, all 483 regulons are organized into 13 modules. Representative regulators and cell clusters were identified in each module. For example, module 3 was consisted of hypertrophic chondrocytes and chondrocytes, containing regulons of ERF, BHL, HE41, FOXC1, HE40 and ATF2. Module 5 was organized by MSCs and TSCs, including ZNF607, MSX1, ZNF157, GLI2 and ALX4. Module 10 consists of hypertrophic chondrocytes and osteoblasts, containing regulons of PHOX2A, ESRRA, PGAM2 and SOX8 (Fig. 5c). Heatmap shows that many common regulons were turned on between MSCs and TSCs (Fig. 5b). Interaction mapping of transcription factor networks showed that PAX1 and PAX9, which were essential regulators for chondrocyte differentiation, were commonly turned on between MSCs and TSCs. NRF1, TFEB, ALX4 and DLX2, which were associated with MSCs differentiation into osteoblasts, were also commonly turned on between MSCs and TSCs. Additionally, the sequences on the promoter region of transcription factors for target genes including PAX1, PAX9, NRF1, TFEB, ALX4 and DLX2 were also shown (Fig. 5d).

Discussion

To better understand the cell types and differentiation relationship of human embryonic TMJ cells, we have constructed the cell development atlas of 3 and 4-month-old TMJ by single-cell sequencing. In previous reports, many studies have revealed the development of TMJ through imaging and morphological studying[5]. So far, there is no study on the cell level of human embryonic TMJ. This is the first and earliest cell development atlas of human embryonic TMJ. We have identified 15 cell clusters (Fig. 1a). We found that the chondrocytes cluster has not differentiated yet in 3-month-old TMJ. However, an obvious chondrocytes cluster appeared in 4-month-old TMJ (Fig. 1b and 1c). Therefore, we speculated that chondrocytes differentiated in 4-month-old TMJ. The differentiation of chondrocytes was later than other cell clusters, suggesting that the completion of chondrocytes differentiation occurred in the late development stage of TMJ. This phenomenon is firstly reported in the development of human embryonic TMJ.

We identified a novel cell cluster of TSCs, which could be divided into five subpopulations including osteoblasts, preosteoblasts, hypertrophic chondrocytes, chondrocytes and mesenchymal stem cells (Fig. 2a). The variable compositions of TSCs suggested that TSCs possessed multiple differentiation potentials. Based on this prediction, three novel differentiation lineages which were related to TSCs were proposed by trajectory and RNA velocity analysis. MSCs differentiated into TSCs. TSCs could further differentiate into tenocytes, hypertrophic chondrocytes and osteoblasts (Fig. 3a and 3b). It has been reported that MSCs can differentiate into tenocytes [19]. Inconsistent with previous reports [19], tenocytes are not directly differentiated from MSCs, but from TSCs in human embryonic TMJ (Fig. 3a). During the development process, hypertrophic chondrocytes and osteoblasts were reported as separate cell lineages[6]. They were differentiated from osteochondro-progenitors. Sox9 and Runx2 were higly expressed in osteochondro-progenitors[20]. In this study, similar to osteochondro-progenitors, TSCs highly expressed Sox9 and Runx2 and could differentiate into hypertrophic chondrocytes and osteoblasts, respectively (Fig. 3c). Moreover, RUNX2[21] was reported to participate in the trans-differentiation of chondrocytes into osteoblasts and promoted osteoblast differentiation. RUNX2 was highly expressed along the differentiation pathway of TSCs to hypertrophic chondrocytes and TSCs to osteoblasts. SOX9 was reported to be a pivotal transcriptional regulator of chondrogenesis[22]. MMP13 was related to the osteogenesis[23]. SOX9 and MMP13 were highly expressed along the differentiation pathway of TSCs to hypertrophic chondrocytes. SOST was associated with the differentiation of bone formation[24]. In this study, SOST was highly expressed in osteoclasts. Other key genes include VEGFA[25], COL10A1[26], MAF[27], CCDC80[28] and SYNE2[29] which are related to bone proliferation and differentiation were widely expressed in MSCs, TSCs, tenocytes, hypertrophic chondrocytes and osteoblasts. These results suggested the key genes which were related to the differentiation of chondrocytes and osteoblast expressed across TMJ clusters (Fig. 3c). These genes could promote the differentiation of human embryonic TMJ cells. Interestingly, we found that TSCs also have the potential ability to differentiate into tenocytes. Therefore, as intermediate cells, TSCs between MSCs and other cell clusters was essential for the development of

human embryonic TMJ. Although we have determined the existing of TSCs in human embryonic TMJ (Fig. 2e), further experiments will be required to disclose their detailed functions.

We performed cell-cell communication analysis among TMJ cell clusters. We found that FGF signal pathway mediated the cell communication among these five clusters (Fig. 4b). Then, we analyzed the strength of FGF signal pathway and found that FGF7-FGFR1 was the main pathway (Fig. 4c and 4d). FGF7 is reported to promote bone formation through increasing osteogenesis [30]. FGF7 also promoted osteogenic differentiation by regulating the expression of β-catenin and Runx2 signaling pathway [31]. In this study, as the source cell cluster, TSCs communicated with the target cell cluster of MSCs by FGF7-FGFR1 signaling pathway. Furthermore, as the source cell clusters, tenocytes, hypertrophic chondrocytes and osteoblasts communicated with the target cell cluster of TSCs also by FGF7-FGFR1 signaling pathway, respectively. Therefore, as the main signal pathway, we determined that FGF7-FGFR1 mediated the communication and differentiation among MSCs, TSCs, tenocytes, hypertrophic chondrocytes and osteoblasts. In addition, we also explored other signaling pathways among TSCs, hypertrophic chondrocytes and osteoblasts. Notably, many differentiation signaling pathways of chondrocytes and osteoblasts were screened including PTN [13], BMP [14], TENASCIN [32], ACTIVIN[33], RANKL[33], DMP1 [34], MK [35], FGF [15], GRN [36], CXCL [16], MSTN[17] and GH [18]. These reported signaling pathways regulating bone differentiation may also play important roles in the differentiation of TSCs, hypertrophic chondrocytes and osteoblasts. In addition, we screened other signaling pathways including THBS, ANGPTL, CHAD, CADM, CDH, BSP, HSPG, OSM, ncWNT, SEMA4, IL16 and so on, which also mediated the cell communication of TSCs, hypertrophic chondrocytes and osteoblasts (Fig. 4e). The roles of these signaling pathways in the cell differentiation are elusive and need to be further explored.

Apart from cell-cell communication analysis, transcription factors analysis showed that some specific transcription factors were turned on in the cell clusters (Fig. 5a). For example, SHOX2 [37], TBX18 [38] and PAX9 [39] which were related to the differentiation of ossification and chondroitin were turned on in MSCs. TCF7 [15], DLX6 [40] and MSX1[41] which were reported to participate in the differentiation of ossification and chondroitin were turned on in TSCs. MKX [42] which was related to tendon differentiation was turned on in tenocytes. FOXA2 [43], TRPS1 [44], SOX6 [45] and FOXA3 [46] which were related to the differentiation and hypertrophy of chondrocyte were turned on in hypertrophic chondrocytes. DLX3[47] and IRX5[48] which were associated with the differentiation of ossification were turned on in osteoblasts. These results suggested that the transcription factors which were specifically turned on were crucial for maintaining the specific function in cell clusters. In addition, module analysis revealed that common regulons were turned on across the cell clusters (Fig. 5c). For example, Module 3 consisted hypertrophic chondrocytes and chondrocytes cluster, containing common regulons of ERF[49], FOXC1[50] and ATF2[51] which were reported to participate in the bone formation and osteogenic differentiation. Module 10 was composed of hypertrophic chondrocytes and osteoblasts, containing common regulons of SOX8[52] and ESRRA[53] which were essential regulators for chondrogenic and osteoblast differentiation (Fig. 5c). It is worth noting that common regulon including PAX9 [39], SP9 and TCF7[15,54] were turned on between MSCs and TSCs.

Regulon module analysis showed MSCs and TSCs were in module 5. Thirty-two common regulons further turned on MSCs and TSCs. Among these common regulons, PAX1 [55] and PAX9 were essential regulators for chondrocyte differentiation. NRF1 [56], TFEB [57], ALX4 [58] and DLX2[59] were associated with MSCs differentiating into osteoblasts (Fig. 5d). These common regulons which were turned on between MSCs and TSCs may mediate the differentiation from MSCs into TSCs and further into tenocytes, hypertrophic chondrocytes, and osteoblasts, respectively.

Conclusions

Taken together, our data provided the first and earliest cell development atlas of human embryonic TMJ. The present results demonstrated chondrocytes differentiated in 4-month-old TMJ and the differentiation of chondrocytes was later than other cell clusters. Our results also demonstrated the differentiation relationship and underlying differentiation mechanism among MSCs, TSCs, tenocytes, hypertrophic chondrocytes and osteoblasts by the advanced analysis of single-cell sequencing (Fig. 6). This study is an indispensable resource for investigating the development and differentiation of human embryonic TMJ. Our results also are significant for studying the cellular mechanisms of temporomandibular disorders (TMD) that are caused by abnormal embryonic development of TMJ.

Materials And Methods

Human embryonic TMJ collection

This work was reviewed and approved by the institutional review boards of Affiliated Hospital of Nantong University. Informed consent was signed by the parents of study participants. For scRNA-seq, the TMJ tissues were isolated by surgical resection. A 3 and 4-month-old aborted fetus were used in this study. The TMJ tissues were placed in tissue preservation solution (Singleron Biotechnologies, Nanjing, China) and transported at a low temperature.

The preparation of single-cell suspension

Human embryonic TMJ dissociation was performed according to the previous study[60]. Briefly, separated TMJ tissues were cut into 2–3 mm pieces. The tissue pieces were washed using Hanks Balanced Salt Solution (HBSS). The tissue dissociation solution (Singleron Biotechnologies, Nanjing, China) was used to digest the pieces for 15 min with rotation. They were filtered through a 40-μm sterile strainer (Corning, NY, USA) and centrifuged at 150 g for 5 min. Red blood cells were removed using a lysis reagent (Singleron Biotechnologies, Nanjing, China) for 10 min. After that, the cells were resuspended using PBS and stained with trypan blue (T6146, Sigma, Burlington, VT, USA). The viability of cells was evaluated using a TC20 automated cell counter (Bio-Rad, Hercules, CA, USA).

Library preparation and data preprocessing

The concentration of 1×10^5 cells/mL of cell suspension was then added to the microfluidic plate. The scRNA-seq libraries were constructed using a single-cell RNA library kit (Singleron Biotechnologies, Nanjing, China). The constructed libraries were pooled for the sequencing on the Illumina HiSeq ×10 sequencing machine. Raw reads were processed by CeleScope (https://github.com/singleron-RD/CeleScope) pipeline. Firstly, low quality raw reads and adaptor sequences were trimmed by fastqc (version 0.11.7) and cutadapt (version 1.17). The reads were mapped to GRCm38 (Ensembl V. 92 annotation) using STAR (version 020201). The gene counts and UMI counts were calculated using FeatureCounts (version 1.6.2). The series of analysis procedures were accomplished by CeleScope and the gene expression matrix were generated.

Dimension-reduction and clustering analysis

The dimension reduction and cell clustering were carried out in R with the Seurat version 4 package (https://satijalab.org/seurat/)[61]. The sctransform (SCT) (https://github.com/ChristophH/sctransform) was used to eliminate batch effects and normalize the expression data. The top 3000 variable genes were selected for sample data integration. “FindNeighbors” using 50 dimensions and “FindClusters” using a resolution of 0.25 were used to separate cell clusters. The subcluster analyses of TSCs were set using a resolution of 0.1. The clusters were visualized using the uniform manifold approximation and projection (UMAP) algorithm. For differentially expressed genes (DEGs) analyses, the “FindMarkers” of Seurat was used. The genes which expressed in more than 25% of its cluster and had an average log (Fold Change) expression > 0.25 were defined as DEGs.

Cell type annotation and gene enrichment analyses

The cell-type annotation was according to the expression of known marker genes from published pieces of literature. Subsequently, gene enrichment was performed by clusterProfiler v3.6.1 (https://bioconductor.org/packages/3.11/bioc/html/clusterProfiler.html)[62]. Biological process (BP) with p_adj value < 0.05 were defined as significantly enriched. GO classifications were screened from the org.Hs.eg.db database (https://bioconductor.org/packages/3.11/data/annotation/html/org.Hs.eg.db.html). The GSEABase package (version 1.36.0) was used for Gene Set Enrichment Analysis (GSEA) analyses. The gene sets were downloaded from the Molecular Signatures Database.

Trajectory Analysis and RNA velocity

The pseudotime trajectory of TMJ cell clusters was carried out by Monocle 3 (https://cole-trapnelllab.github.io/monocle3). The highly variable genes were selected from each cluster. The trajectory was visualized using the UMAP method. Finally, the cells were ordered according to the development and differentiation relationship. For RNA velocity analyses, the BAM files containing each cluster were firstly processed into loom files. Subsequently, the loom files were used as an input and processed into a spliced and unspliced matrix. Finally, the results were visualized by the UMAP method.

Cell-cell communication analysis

Cell-cell communication networks by ligand-receptor interaction were analyzed using CellChat (http://www.cellchat.org/; last accessed on May 10, 2021)[63]. A total of 32,491 ligand-receptor pairs were screened from “CellChatDB.human” database. The number of ligand-receptor interactions and interaction strength among TMJ cell clusters was calculated using the function of “computeCommunProb” and “aggregateNet” in CellChat. The major signaling pathways were determined using the function of “computeCommunProbPathway”. The analysis of outgoing communication patterns of secreting cells and incoming communication patterns of target cells was performed using “identifyCommunicationPatterns”.

Transcription factors analysis

The transcription factors analysis was performed using the python version of Single-Cell Regulatory Network Inference and Clustering (pySCENIC)[64]. Cell-type-specific regulons were screened using the regulon specificity score (RSS), which was proposed in a previous study[65]. Regulon module analyses were performed using the parameter of Connection Specificity Index (CSI) which was reported in previous studies[66]. The regulatory network associated with MSCs and TSCs was analyzed using Cytoscape[67].

Immunofluorescent staining

The immunofluorescence procedures were performed according to previous studies[60]. In brief, human embryonic TMJ was fixed with 4% paraformaldehyde at 4℃ for 24 h. The samples were demineralized at 4℃ gently shaking for 2 weeks in 4% EDTA in PBS. The tissue sections with 4 μm thick were cut from TMJ tissues. 10 mM sodium citrate buffer (pH 6.0) was used for the antigen retrieval. Subsequently, sections were blocked in 5% donkey serum containing 0.1% Triton X-100 in 2% BSA. For THBS1 staining, the diluted primary antibody of mouse anti-THBS1 antibody (1:200, Invitrogen, MA5-13398) was added on to the sections and kept at 4˚C overnight. Sections were further incubated in the dark with the secondary antibody (Donkey anti-Rabbit Secondary Antibody, Alexa Fluor 488, Invitrogen, 1:500) for 1 hour at room temperature. For double staining of CAPN6 and PTN, the diluted primary antibody of mouse anti-CAPN6 antibody (1:200, Invitrogen, MA5-24733) and rabbit anti-PTN antibody (1:200, Proteintech, 27117-1-AP) were simultaneously added on to the sections. The secondary antibody (Donkey anti-rabbit secondary antibody, Alexa Fluor 488, Invitrogen, 1:500) and (Donkey anti-mouse secondary antibody, Alexa Fluor 568, Invitrogen, 1:500) were used for the double staining. The nuclei were stained with DAPI for 5 min. The images were captured with Leica SP8 laser scanning confocal microscopy (Leica TCSSP8, Leica).

Declarations

Data availability

The raw data in this study were deposited in the Genome Sequence Archive[68] at the National Genomics Data Center[69], China National Center for Bioinformation/Beijing Institute of Genomics, Chinese Academy

of Sciences (GSA-Human: HRA002545). The cell–gene matrix has been uploaded in “FigShare [https://doi.org/10.6084/ m9.figshare.20407371, https://doi.org/10.6084/m9.figshare.20407383]. All other relevant data supporting the key findings of this study are available within the article and its Supplementary Information files or from the corresponding author upon reasonable request.

Code availability

All code associated with this manuscript have been uploaded to “GitHub [https://github.com/qianqi234/human_embryonic_TMJ]”.

Ethics approval and consent to participate

This work was reviewed and approved by the institutional review boards of Affiliated Hospital of Nantong University. Informed consent was signed by the parents of study participants. For scRNA-seq, the TMJ tissues were isolated by surgical resection. A 3 and 4-month-old aborted fetus were used in this study. The TMJ tissues were placed in tissue preservation solution (Singleron Biotechnologies, Nanjing, China) and transported at a low temperature.

Consent for publication

All authors approved the submitted manuscript.

Availability of data and materials

All data generated or analysed during this study are included in this published article.

Competing interests

The authors declared that there is no conflict of interest associated with this study.

Funding

This work was supported in part by grants from the Nantong City Science and Technology Projects Funds (MS12020030 to X.M.F), Shanghai Wu MengChao Medical Science Foundation (HXKT20200019 to X.M.F), Jiangsu Yancheng Timstar Medical Technology Co., Ltd (HXKT20211014 to X.M.F, HXKT20211018 to X.M.F), Natural Science Foundation of Nantong (JC2021081 to J.W.S), Funing Meite Dental Materials Factory (ZZXM-20201009 to X.M.F, ZZXM-20201008 to C.F.W), National Natural Science Foundation of China (2018YFA0801004 and 81870359 to D.L), Natural Science Foundation of Jiangsu Province (BK20180048, and BRA2019278 to D.L).National Natural Science Foundation of China (82001606 to C.N.W.), National Natural Science Foundation of China (82071838 to Z.F.G).-

Authors' contributions

Conceived and designed the experiments: X.M.F, J.W.S, D.L and G.F.Z; Performed the experiments: Q.Q.Z, M.Y.T, J.P.H, L.L, R.R.J, X.D.F and L.W; Analyzed the data: C.F.W, H.M.X, J.Q.Z, Y.J.G, Y.Q.G; Wrote the

paper: Q.Q.Z, M.Y.T and C.N.W.

Acknowledgements

We thank all members of the laboratory for their experimental assistance and constructive discussion.

Authors' information

[1]Department of Stomatology, Affiliated Hospital of Nantong University, Medical School of Nantong University, Nantong, 226001, China;

[2]Research Center of Clinical Medicine, Affiliated Hospital of Nantong University, Medical School of Nantong University, Nantong, 226001, China;

[3]Institute of Reproductive Medicine, Medical School of Nantong University, Nantong, 226001, China;

[4]School of Life Science, Nantong Laboratory of Development and Diseases; Second Affiliated Hospital; Key Laboratory of Neuroregeneration of Jiangsu and Ministry of Education, Co-innovation Center of Neuroregeneration, Nantong University, Nantong, 226019, China.

References

1. Gauer, R. L. & Semidey, M. J. Diagnosis and treatment of temporomandibular disorders. *Am Fam Physician* **91**, 378-386 (2015).
2. Stocum, D. L. & Roberts, W. E. Part I: Development and Physiology of the Temporomandibular Joint. *Curr Osteoporos Rep* **16**, 360-368, doi:10.1007/s11914-018-0447-7 (2018).
3. Zarb, G. A. & Carlsson, G. E. Temporomandibular disorders: osteoarthritis. *J Orofac Pain* **13**, 295-306 (1999).
4. Bender, M. E., Lipin, R. B. & Goudy, S. L. Development of the Pediatric Temporomandibular Joint. *Oral Maxillofac Surg Clin North Am* **30**, 1-9, doi:10.1016/j.coms.2017.09.002 (2018).
5. Merida-Velasco, J. R. *et al.* Development of the human temporomandibular joint. *Anat Rec* **255**, 20-33, doi:10.1002/(SICI)1097-0185(19990501)255:1<20::AID-AR4>3.0.CO;2-N (1999).
6. Karsenty, G., Kronenberg, H. M. & Settembre, C. Genetic control of bone formation. *Annu Rev Cell Dev Biol* **25**, 629-648, doi:10.1146/annurev.cellbio.042308.113308 (2009).
7. Akiyama, H. *et al.* Osteo-chondroprogenitor cells are derived from Sox9 expressing precursors. *Proc Natl Acad Sci U S A* **102**, 14665-14670, doi:10.1073/pnas.0504750102 (2005).
8. Akiyama, H., Chaboissier, M. C., Martin, J. F., Schedl, A. & de Crombrugghe, B. The transcription factor Sox9 has essential roles in successive steps of the chondrocyte differentiation pathway and is required for expression of Sox5 and Sox6. *Genes Dev* **16**, 2813-2828, doi:10.1101/gad.1017802 (2002).

9. Hirata, M. *et al.* C/EBPbeta and RUNX2 cooperate to degrade cartilage with MMP-13 as the target and HIF-2alpha as the inducer in chondrocytes. *Hum Mol Genet* **21**, 1111-1123, doi:10.1093/hmg/ddr540 (2012).
10. Nakashima, K. *et al.* The novel zinc finger-containing transcription factor osterix is required for osteoblast differentiation and bone formation. *Cell* **108**, 17-29, doi:10.1016/s0092-8674(01)00622-5 (2002).
11. Lum, L. & Beachy, P. A. The Hedgehog response network: sensors, switches, and routers. *Science* **304**, 1755-1759, doi:10.1126/science.1098020 (2004).
12. Becher, C. *et al.* Decrease in the expression of the type 1 PTH/PTHrP receptor (PTH1R) on chondrocytes in animals with osteoarthritis. *J Orthop Surg Res* **5**, 28, doi:10.1186/1749-799X-5-28 (2010).
13. Jin, L. *et al.* Pleiotropin enhances the osteo/dentinogenic differentiation potential of dental pulp stem cells. *Connect Tissue Res* **62**, 495-507, doi:10.1080/03008207.2020.1779238 (2021).
14. Zhu, L. *et al.* Application of BMP in Bone Tissue Engineering. *Front Bioeng Biotechnol* **10**, 810880, doi:10.3389/fbioe.2022.810880 (2022).
15. Komori, T. Regulation of Proliferation, Differentiation and Functions of Osteoblasts by Runx2. *Int J Mol Sci* **20**, doi:10.3390/ijms20071694 (2019).
16. Liu, C. *et al.* CXCL12/CXCR4 signal axis plays an important role in mediating bone morphogenetic protein 9-induced osteogenic differentiation of mesenchymal stem cells. *Int J Med Sci* **10**, 1181-1192, doi:10.7150/ijms.6657 (2013).
17. Suh, J. *et al.* GDF11 promotes osteogenesis as opposed to MSTN, and follistatin, a MSTN/GDF11 inhibitor, increases muscle mass but weakens bone. *Proc Natl Acad Sci U S A* **117**, 4910-4920, doi:10.1073/pnas.1916034117 (2020).
18. Darvin, P., Joung, Y. H. & Yang, Y. M. JAK2-STAT5B pathway and osteoblast differentiation. *JAKSTAT* **2**, e24931, doi:10.4161/jkst.24931 (2013).
19. Fang, W., Sun, Z., Chen, X., Han, B. & Vangsness, C. T., Jr. Synovial Fluid Mesenchymal Stem Cells for Knee Arthritis and Cartilage Defects: A Review of the Literature. *J Knee Surg* **34**, 1476-1485, doi:10.1055/s-0040-1710366 (2021).
20. Mackie, E. J., Ahmed, Y. A., Tatarczuch, L., Chen, K. S. & Mirams, M. Endochondral ossification: how cartilage is converted into bone in the developing skeleton. *Int J Biochem Cell Biol* **40**, 46-62, doi:10.1016/j.biocel.2007.06.009 (2008).
21. Qin, X. *et al.* Runx2 is essential for the transdifferentiation of chondrocytes into osteoblasts. *PLoS Genet* **16**, e1009169, doi:10.1371/journal.pgen.1009169 (2020).
22. Dalle Carbonare, L. *et al.* Modulation of miR-204 Expression during Chondrogenesis. *Int J Mol Sci* **23**, doi:10.3390/ijms23042130 (2022).
23. Arai, Y. *et al.* Cryptic ligand on collagen matrix unveiled by MMP13 accelerates bone tissue regeneration via MMP13/Integrin alpha3/RUNX2 feedback loop. *Acta Biomater* **125**, 219-230, doi:10.1016/j.actbio.2021.02.042 (2021).

24. Delgado-Calle, J., Sato, A. Y. & Bellido, T. Role and mechanism of action of sclerostin in bone. *Bone* **96**, 29-37, doi:10.1016/j.bone.2016.10.007 (2017).
25. Wang, X. *et al.* Fluid shear stress-induced down-regulation of microRNA-140-5p promotes osteoblast proliferation by targeting VEGFA via the ERK5 pathway. *Connect Tissue Res* **63**, 156-168, doi:10.1080/03008207.2021.1891228 (2022).
26. Bian, H. *et al.* Expression Profiling and Functional Analysis of Candidate Col10a1 Regulators Identified by the TRAP Program. *Front Genet* **12**, 683939, doi:10.3389/fgene.2021.683939 (2021).
27. Nishikawa, K. *et al.* Maf promotes osteoblast differentiation in mice by mediating the age-related switch in mesenchymal cell differentiation. *J Clin Invest* **120**, 3455-3465, doi:10.1172/JCI42528 (2010).
28. Liu, Y. *et al.* URB expression in human bone marrow stromal cells and during mouse development. *Biochem Biophys Res Commun* **322**, 497-507, doi:10.1016/j.bbrc.2004.07.161 (2004).
29. Mross, C. *et al.* Depletion of Nesprin-2 is associated with an embryonic lethal phenotype in mice. *Nucleus* **9**, 503-515, doi:10.1080/19491034.2018.1523664 (2018).
30. Poudel, S. B. *et al.* Local delivery of recombinant human FGF7 enhances bone formation in rat mandible defects. *J Bone Miner Metab* **35**, 485-496, doi:10.1007/s00774-016-0784-5 (2017).
31. Jeon, Y. M. *et al.* Fibroblast growth factor-7 facilitates osteogenic differentiation of embryonic stem cells through the activation of ERK/Runx2 signaling. *Mol Cell Biochem* **382**, 37-45, doi:10.1007/s11010-013-1716-5 (2013).
32. Tucker, R. P. & Degen, M. The Expression and Possible Functions of Tenascin-W During Development and Disease. *Front Cell Dev Biol* **7**, 53, doi:10.3389/fcell.2019.00053 (2019).
33. Omi, M., Kaartinen, V. & Mishina, Y. Activin A receptor type 1-mediated BMP signaling regulates RANKL-induced osteoclastogenesis via canonical SMAD-signaling pathway. *J Biol Chem* **294**, 17818-17836, doi:10.1074/jbc.RA119.009521 (2019).
34. Yan, X. *et al.* ERalpha/beta/DMP1 axis promotes trans-differentiation of chondrocytes to bone cells through GSK-3beta/beta-catenin pathway. *J Anat*, doi:10.1111/joa.13612 (2022).
35. Emmakah, A. M. *et al.* Megakaryocytes Enhance Mesenchymal Stromal Cells Proliferation and Inhibit Differentiation. *J Cell Biochem*, doi:10.1002/jcb.26289 (2017).
36. Noguchi, T. *et al.* Progranulin plays crucial roles in preserving bone mass by inhibiting TNF-alpha-induced osteoclastogenesis and promoting osteoblastic differentiation in mice. *Biochem Biophys Res Commun* **465**, 638-643, doi:10.1016/j.bbrc.2015.08.077 (2015).
37. Gross, S., Krause, Y., Wuelling, M. & Vortkamp, A. Hoxa11 and Hoxd11 regulate chondrocyte differentiation upstream of Runx2 and Shox2 in mice. *PLoS One* **7**, e43553, doi:10.1371/journal.pone.0043553 (2012).
38. Haraguchi, R., Kitazawa, R. & Kitazawa, S. Epigenetic regulation of Tbx18 gene expression during endochondral bone formation. *Cell Tissue Res* **359**, 503-512, doi:10.1007/s00441-014-2028-0 (2015).

39. Rodrigo, I., Hill, R. E., Balling, R., Munsterberg, A. & Imai, K. Pax1 and Pax9 activate Bapx1 to induce chondrogenic differentiation in the sclerotome. *Development* **130**, 473-482, doi:10.1242/dev.00240 (2003).
40. Komori, T. Regulation of osteoblast differentiation by transcription factors. *J Cell Biochem* **99**, 1233-1239, doi:10.1002/jcb.20958 (2006).
41. Zhou, S. *et al.* STAT3 is critical for skeletal development and bone homeostasis by regulating osteogenesis. *Nat Commun* **12**, 6891, doi:10.1038/s41467-021-27273-w (2021).
42. Chen, G. *et al.* Mkx mediates tenogenic differentiation but incompletely inhibits the proliferation of hypoxic MSCs. *Stem Cell Res Ther* **12**, 426, doi:10.1186/s13287-021-02506-3 (2021).
43. Bell, N. *et al.* Overexpression of transcription factor FoxA2 in the developing skeleton causes an enlargement of the cartilage hypertrophic zone, but it does not trigger ectopic differentiation in immature chondrocytes. *Bone* **160**, 116418, doi:10.1016/j.bone.2022.116418 (2022).
44. Michikami, I. *et al.* Trps1 is necessary for normal temporomandibular joint development. *Cell Tissue Res* **348**, 131-140, doi:10.1007/s00441-012-1372-1 (2012).
45. Yang, Z. *et al.* miR-23a-3p regulated by LncRNA SNHG5 suppresses the chondrogenic differentiation of human adipose-derived stem cells via targeting SOX6/SOX5. *Cell Tissue Res* **383**, 723-733, doi:10.1007/s00441-020-03289-4 (2021).
46. Amano, K., Densmore, M., Nishimura, R. & Lanske, B. Indian hedgehog signaling regulates transcription and expression of collagen type X via Runx2/Smads interactions. *J Biol Chem* **289**, 24898-24910, doi:10.1074/jbc.M114.570507 (2014).
47. Lee, S. H., Oh, K. N., Han, Y., Choi, Y. H. & Lee, K. Y. Estrogen Receptor alpha Regulates Dlx3-Mediated Osteoblast Differentiation. *Mol Cells* **39**, 156-162, doi:10.14348/molcells.2016.2291 (2016).
48. Tan, Z. *et al.* IRX3 and IRX5 Inhibit Adipogenic Differentiation of Hypertrophic Chondrocytes and Promote Osteogenesis. *J Bone Miner Res* **35**, 2444-2457, doi:10.1002/jbmr.4132 (2020).
49. Vogiatzi, A. *et al.* Erf Affects Commitment and Differentiation of Osteoprogenitor Cells in Cranial Sutures via the Retinoic Acid Pathway. *Mol Cell Biol* **41**, e0014921, doi:10.1128/MCB.00149-21 (2021).
50. Zhang, L. *et al.* MiR-138-5p knockdown promotes osteogenic differentiation through FOXC1 up-regulation in human bone mesenchymal stem cells. *Biochem Cell Biol* **99**, 296-303, doi:10.1139/bcb-2020-0163 (2021).
51. Zhang, H. *et al.* LncRNA NEAT1 controls the lineage fates of BMSCs during skeletal aging by impairing mitochondrial function and pluripotency maintenance. *Cell Death Differ* **29**, 351-365, doi:10.1038/s41418-021-00858-0 (2022).
52. Herlofsen, S. R. *et al.* Brief report: importance of SOX8 for in vitro chondrogenic differentiation of human mesenchymal stromal cells. *Stem Cells* **32**, 1629-1635, doi:10.1002/stem.1642 (2014).
53. Auld, K. L. *et al.* Estrogen-related receptor alpha regulates osteoblast differentiation via Wnt/beta-catenin signaling. *J Mol Endocrinol* **48**, 177-191, doi:10.1530/JME-11-0140 (2012).

54. Mikasa, M. *et al.* Regulation of Tcf7 by Runx2 in chondrocyte maturation and proliferation. *J Bone Miner Metab* **29**, 291-299, doi:10.1007/s00774-010-0222-z (2011).
55. Sivakamasundari, V. *et al.* A developmental transcriptomic analysis of Pax1 and Pax9 in embryonic intervertebral disc development. *Biol Open* **6**, 187-199, doi:10.1242/bio.023218 (2017).
56. Liu, Z. *et al.* CNC-bZIP protein NFE2L1 regulates osteoclast differentiation in antioxidant-dependent and independent manners. *Redox Biol* **48**, 102180, doi:10.1016/j.redox.2021.102180 (2021).
57. Pastore, N. *et al.* TFEB regulates murine liver cell fate during development and regeneration. *Nat Commun* **11**, 2461, doi:10.1038/s41467-020-16300-x (2020).
58. Antonopoulou, I., Mavrogiannis, L. A., Wilkie, A. O. & Morriss-Kay, G. M. Alx4 and Msx2 play phenotypically similar and additive roles in skull vault differentiation. *J Anat* **204**, 487-499, doi:10.1111/j.0021-8782.2004.00304.x (2004).
59. Zeng, X., Wang, Y., Dong, Q., Ma, M. X. & Liu, X. D. DLX2 activates Wnt1 transcription and mediates Wnt/beta-catenin signal to promote osteogenic differentiation of hBMSCs. *Gene* **744**, 144564, doi:10.1016/j.gene.2020.144564 (2020).
60. Shi, J. *et al.* Spatio-temporal landscape of mouse epididymal cells and specific mitochondria-rich segments defined by large-scale single-cell RNA-seq. *Cell Discov* **7**, 34, doi:10.1038/s41421-021-00260-7 (2021).
61. Stuart, T. *et al.* Comprehensive Integration of Single-Cell Data. *Cell* **177**, 1888-1902 e1821, doi:10.1016/j.cell.2019.05.031 (2019).
62. Yu, G., Wang, L. G., Han, Y. & He, Q. Y. clusterProfiler: an R package for comparing biological themes among gene clusters. *OMICS* **16**, 284-287, doi:10.1089/omi.2011.0118 (2012).
63. Jin, S. *et al.* Inference and analysis of cell-cell communication using CellChat. *Nat Commun* **12**, 1088, doi:10.1038/s41467-021-21246-9 (2021).
64. Aibar, S. *et al.* SCENIC: single-cell regulatory network inference and clustering. *Nat Methods* **14**, 1083-1086, doi:10.1038/nmeth.4463 (2017).
65. Suo, S. *et al.* Revealing the Critical Regulators of Cell Identity in the Mouse Cell Atlas. *Cell Rep* **25**, 1436-1445 e1433, doi:10.1016/j.celrep.2018.10.045 (2018).
66. Fuxman Bass, J. I. *et al.* Using networks to measure similarity between genes: association index selection. *Nat Methods* **10**, 1169-1176, doi:10.1038/nmeth.2728 (2013).
67. Shannon, P. *et al.* Cytoscape: a software environment for integrated models of biomolecular interaction networks. *Genome Res* **13**, 2498-2504, doi:10.1101/gr.1239303 (2003).
68. Chen, T. *et al.* The Genome Sequence Archive Family: Toward Explosive Data Growth and Diverse Data Types. *Genomics Proteomics Bioinformatics* **19**, 578-583, doi:10.1016/j.gpb.2021.08.001 (2021).
69. Members, C.-N. & Partners. Database Resources of the National Genomics Data Center, China National Center for Bioinformation in 2021. *Nucleic Acids Res* **49**, D18-D28, doi:10.1093/nar/gkaa1022 (2021).

Figures

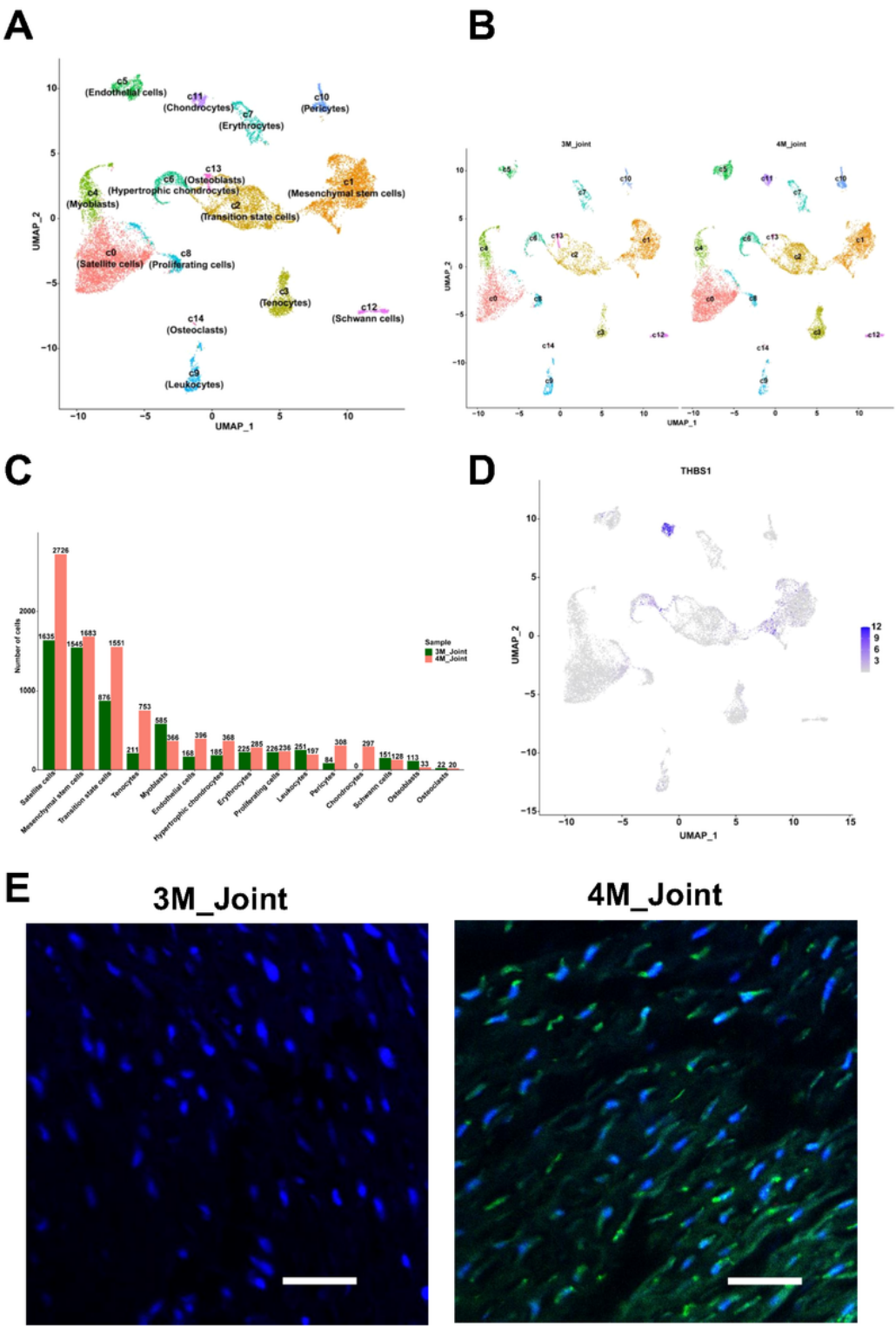

Figure 1

Overview of the scRNA sequencing of human embryonic TMJ. A The 15 cell clusters identified in human embryonic TMJ using UMAP. B The cell clusters were identified in 3 and 4-month-old human embryonic TMJ. C The statistics of cells in each cluster from 3 and 4-month-old human embryonic TMJ. D The

expression of THBS1 in each cluster of human embryonic TMJ. E The immunofluorescent staining of THBS1 in 3 and 4-month-old human embryonic TMJ, green: THBS1, blue: DAPI, Scale bar = 50 μm.

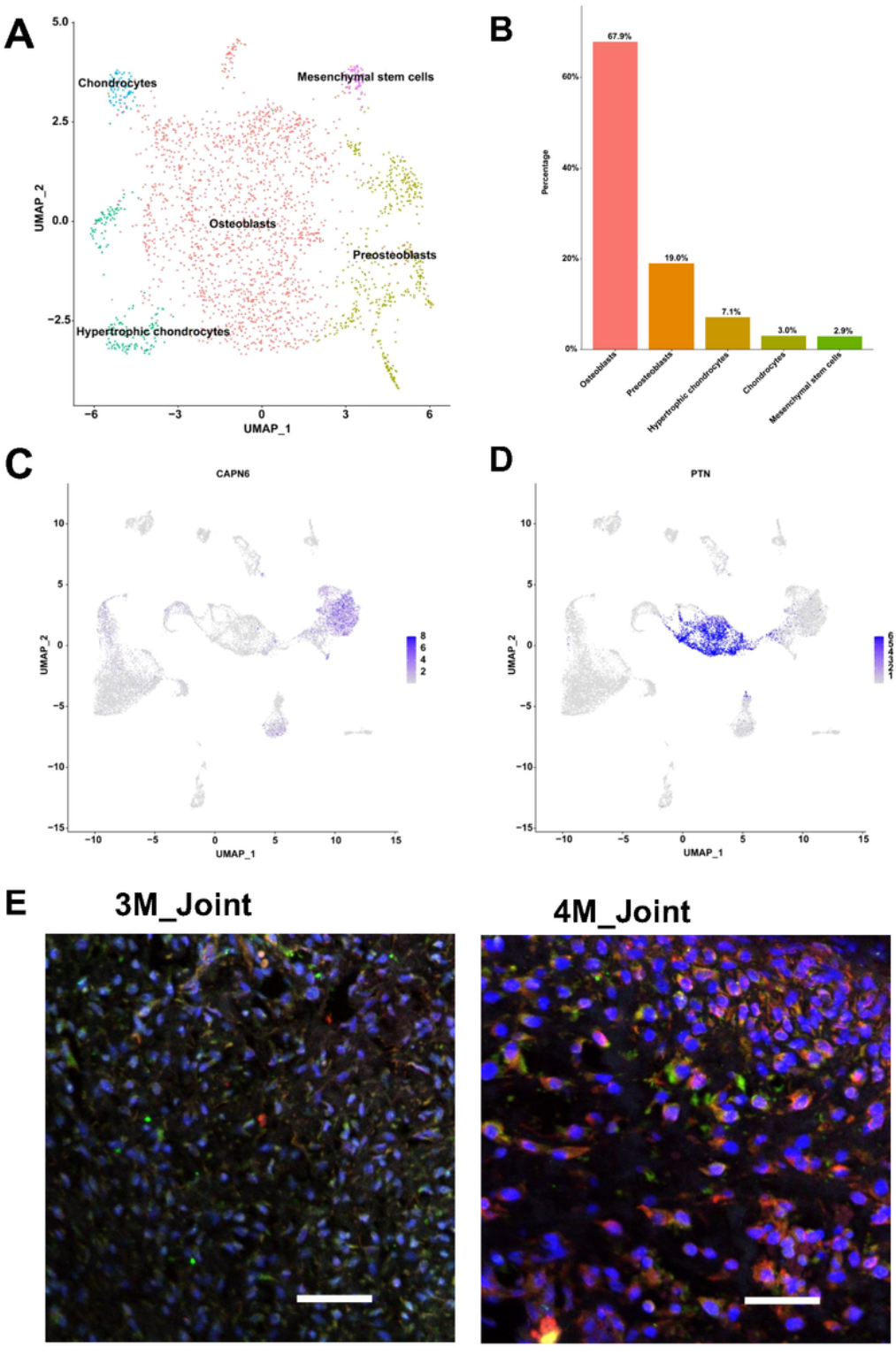

Figure 2

Subpopulation analysis of TSCs. A The five subpopulations of TSCs were visualized using UMAP. B The cell proportions of subpopulations in TSCs. C The expression of CAPN6 in each cluster of human

embryonic TMJ. D The expression of PTN in each cluster of human embryonic TMJ. E Immunofluorescence staining of CAPN6 and PTN in 3 and 4-month-old human embryonic TMJ, green: PTN, red: CAPN6, blue: DAPI, Scale bar = 50 μm.

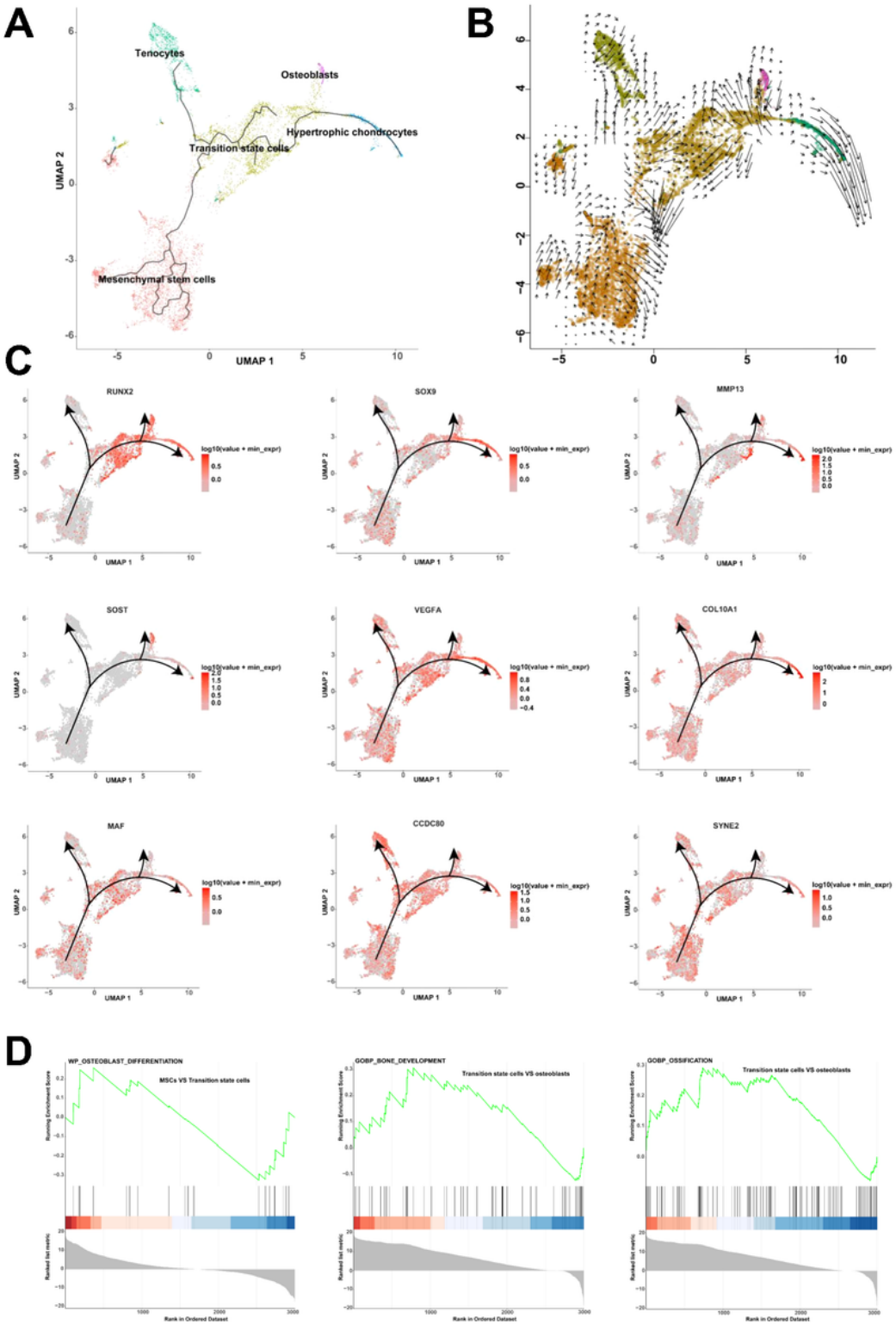

Figure 3

The differentiation relationship analysis of MSCs, TSCs, tenocytes, hypertrophic chondrocytes and osteoblasts. A The differentiation relationship among MSCs, TSCs, tenocytes, hypertrophic chondrocytes and osteoblasts based on Monocle3 analysis. B The differentiation relationship among these five clusters based on RNA velocity analysis. C The expression of key genes including RUNX2, SOX9, MMP13, SOST, VEGFA, COL10A1, MAF, CCDC80 and SYNE2 among the five clusters. D GSEA analysis among MSCs, TSCs and osteoblasts.

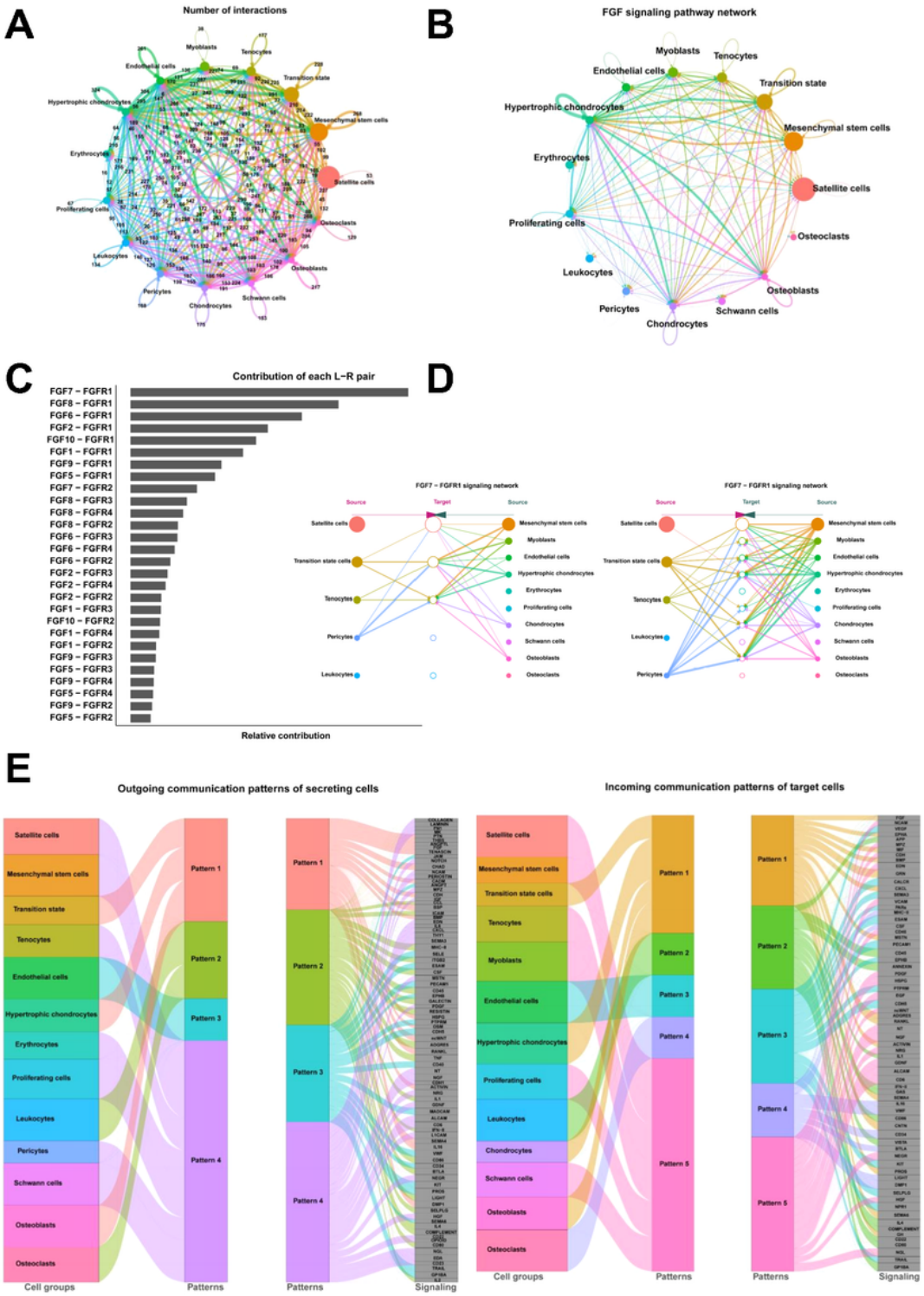

Figure 4

CellChat analysis of human embryonic TMJ clusters. A The number of ligand-receptor pairs in 15 cell clusters. B FGF signaling pathway networks among 15 cell clusters. C The contribution of each ligand-receptor pairs of FGF signaling pathway. D FGF7-FGFR1 signaling pathway networks among 15 cell clusters. E The analysis of outgoing communication patterns of secreting cells and incoming communication patterns of target cells among 15 cell clusters.

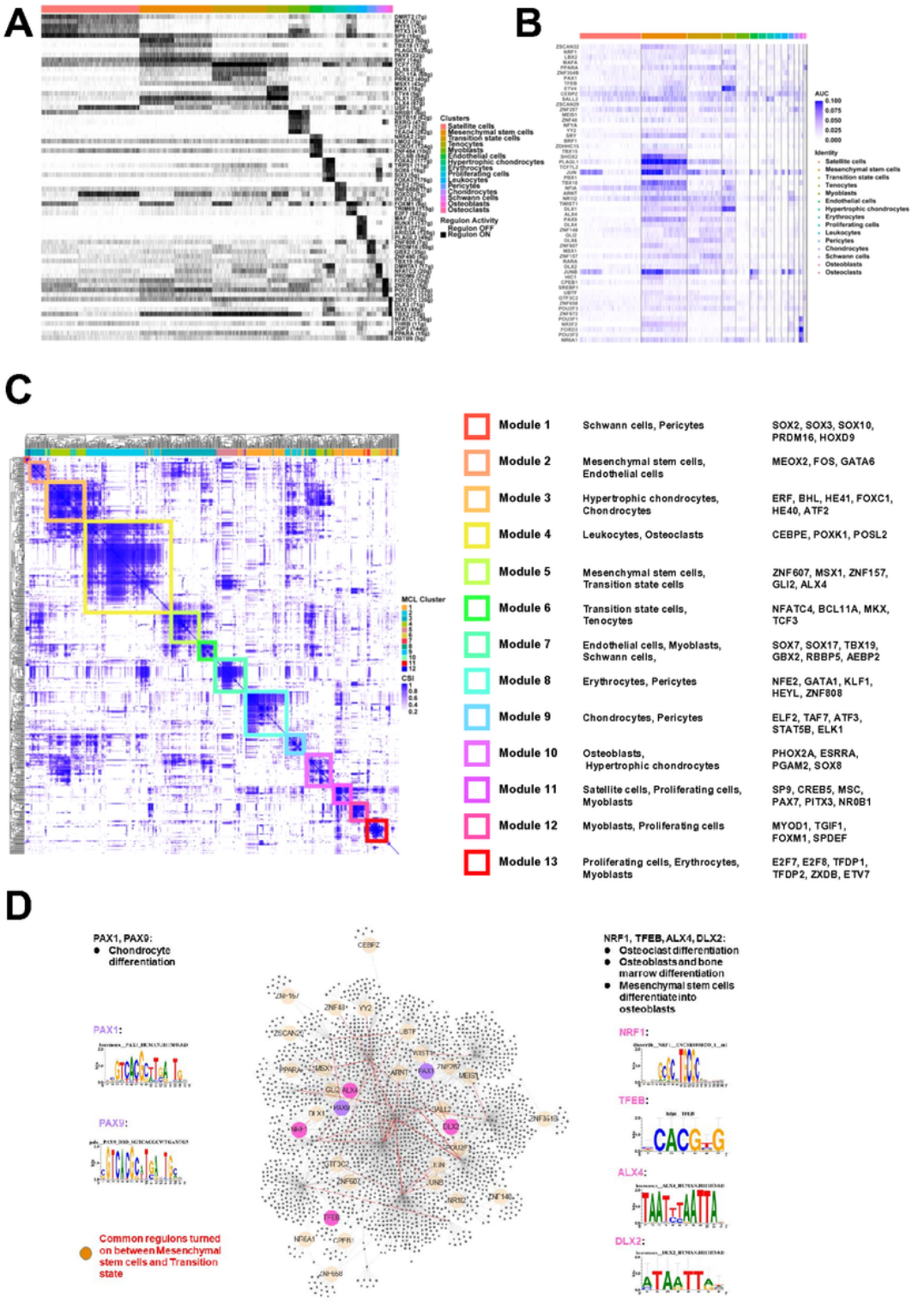

Figure 5

Transcription factors analysis among human embryonic TMJ clusters. A The regulon activity analysis showed the on/off of the specific regulons in each cluster. B Heatmap showed the common regulons were turned on between MSCs and TSCs. C Modules analysis of cell clusters and common regulons. D Interaction mapping of transcription factors networks showed common regulons between MSCs and TSCs.

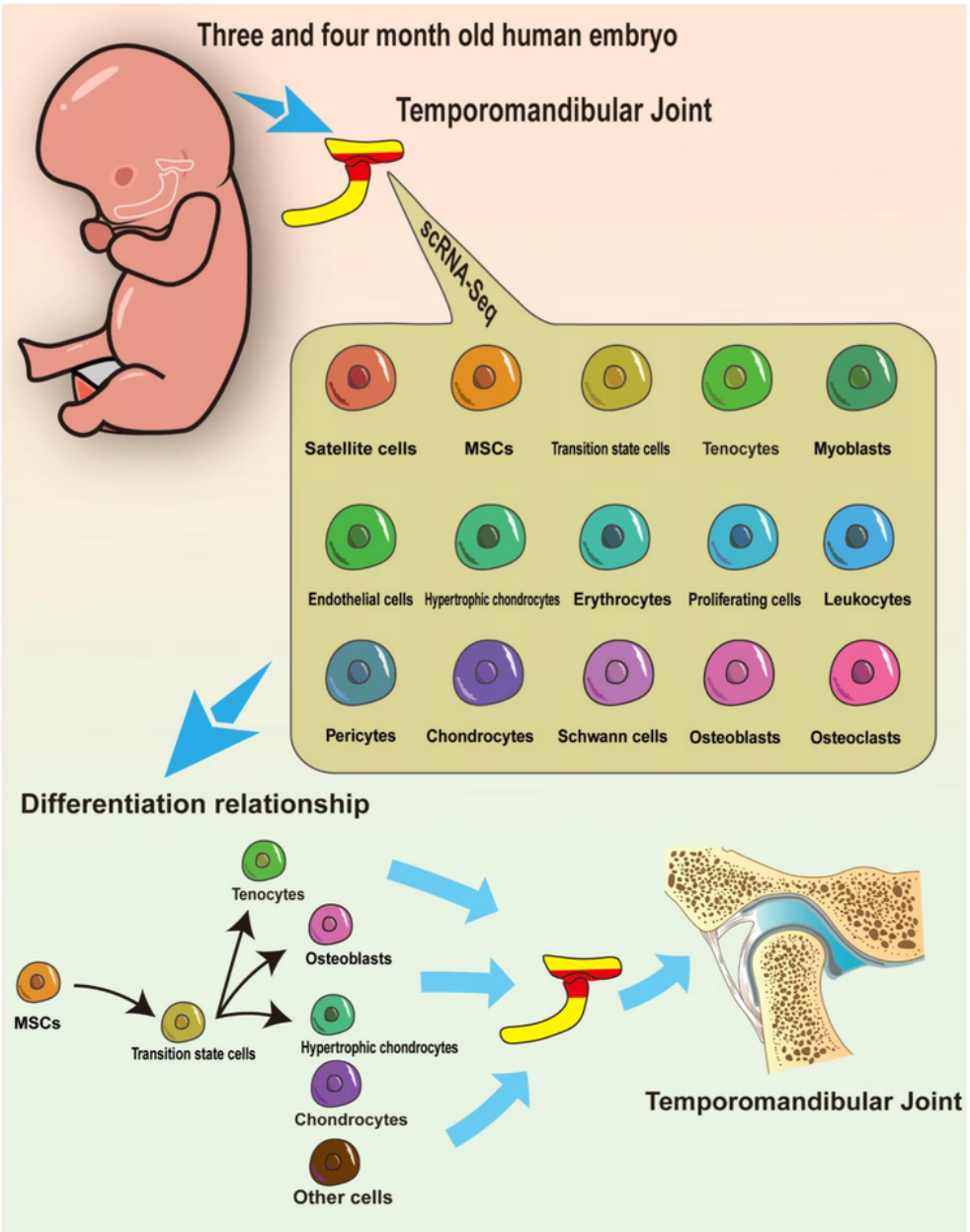

Figure 6

Overview of the cell types and differentiation relationship among human embryonic TMJ cells.

Supplementary Files

This is a list of supplementary files associated with this preprint. Click to download.

- renamed7663a7.png
- renamed7663a8.png
- renamed7663a9.png
- renamed7663a10.png